SLAG FURNACES - SOME ISSUES FOR OPTIMAL DESIGN AND OPERATION

Mark William Kennedy

Proval Partners SA
70 Rue de Genève
1004 Lausanne
Switzerland
m.kennedy@provalp.com

Keywords: Slag, Furnace, Power, Design, Efficiency

Abstract

'Rules-of-thumb', some of which were originally intended for arc furnaces, play a significant role in the design process for slag containing furnaces. Lack of fundamental understanding of the physics driving the performance of these furnaces sometimes results in either overly conservative, or poorly performing designs. This paper will explore some key technical issues related to the correct design and optimal operation of slag furnaces. Reference will be made to both traditional and non-traditional designs to emphasise the potential room for continued development.

Introduction

Slag containing furnaces are important metallurgical vessels for smelting, converting and slag cleaning. Slag furnaces are used in the processing of iron and ferroalloys [1], as well as non-ferrous metals, e.g. copper [2], nickel [3], zinc [4], Precious Group Metals (PGM's) [5], etc. Energy sources in slag furnaces typically include: (i) electrical, (ii) oxidation of sulphur or iron in the feed, and (iii) combustion of hydrocarbons. The focus of this paper will be on furnaces used for smelting and that derive a significant portion of the total input energy from direct or indirect heating of the slag with electricity.

Some issues related to electrically powered slag furnaces will be discussed and related to their impact on optimal furnace design and operation:

1. Process intensity.
2. Basic dimensioning.
3. Conversion of electrical energy into heat.
4. Transfer of sensible heat to charge and wall.
5. Impact of operating practices on furnace efficiency.
6. Influence of the nature of the feed.
7. Volumetric heat sinks and their significant impact on maximum useable power intensity.

Process Intensity

The maximum power intensity that can be efficiently used in a given process is perhaps the most fundamental parameter in the design of a furnace. Furnace power intensity is often written as a flux (kW/m^2) expressed relative to the projected hearth area [6]. Furnace power intensity stated in this way, has increased in stages from <100 kW/m^2 to values occasionally exceeding 400 kW/m^2 in non-ferrous smelting vessels today [7]. As process intensity has increased, so have sidewall heat fluxes. Higher sidewall heat fluxes have had significant negative effects on refractory life. Equipment improvements have been necessary in order to maintain vessel integrity and extend furnace campaign life, e.g. cooled copper structures to maintain sidewall refractory and/or a freeze-lining [8].

The kW/m^2 concept is highly applicable for processes where the use of energy is primarily for the heating and melting of the charge, i.e. providing the sensible heat and net heat of fusion/mixing required to melt the feed material. These processes can be envisaged as being driven by the heat transfer across the projected slag-charge interfacial area. This concept has also been applied to furnaces that have an open bath with minimal or no charge cover, and to furnaces which are wall fed, having open central zones. It is further applied to furnaces operating with shielded or covered arcs, where heat transfer also takes place directly between the arc and the charge.

Alternatively, process intensity can be expressed as a volumetric power density (kW/m^3) as developed for pure 'bath' power Elkem Multi-Purpose Furnace®s using deeply immersed electrodes (see Table I [7]). The idea of volumetric power density is not well accepted in the field of electric furnace engineering. Volumetric power density can be shown to be appropriate for furnaces operating with a high proportion of the total energy input driving reactions that take place on a 'volumetric' basis, e.g. reduction or fuming.

Table I – Volumetric Power Intensity of Elkem Multi-Purpose Furnace®s [7]

Intensity	**Reaction or Slag Zone (kW of bath power/m^3 of slag)**
Normal	100 – 400
High	500 – 1500
Ultra High	1500 – 5000

Given that a typical slag furnace bath is of the order of 1 m deep, there exists a fundamental disconnect between processes which track power intensity on the projected hearth basis, i.e. of the order of 100-400 kW/m^2 or m^3 (assuming a 1 m depth) and those using High, 500-1500 kW/m^3 or Ultra-High, 1500-5000 kW/m^3, volumetric intensities. Although many working in the field of non-ferrous smelting might assume these High/Ultra-High volumetric intensities to be impossible to achieve in practice, an actual example of industrial operation with plasma zinc fuming will be discussed in some detail later. This will be done in order to challenge preconceived notions of what is or is not possible to accomplish in a slag smelting furnace.

Dimensioning – Example of Round Furnaces

The total power requirement and 'intensity' are probably the two most important factors driving the design of a slag furnace. Together these parameters establish the total furnace area. Higher intensity furnaces typically have larger wall heat fluxes, but lower total losses due to the reduced external surface area. Therefore, there typically exists both a capital, and operating benefit from high intensity operation, if it can be accomplished in practice.

Combining the total power input and intensity with electrical or other equipment limitations (e.g. maximum electrode current density or size) and standard scaling ratios leads directly to the basic furnace dimensions including: furnace bath diameter, electrode size, spacing, type and number [9]. Use of high power graphite electrodes and standard scaling ratios, will lead inevitably to a high intensity furnace design. Electric slag furnace dimensioning has been extensively reviewed elsewhere [7, 9, 10]; some key design information will be summarized in this section for round furnaces.

Electric slag furnaces, including those using immersed electrodes, i.e. operating without arcs, have been dimensioned primarily using criteria established from arc furnace design. This is most likely due to the greater prevalence of arc furnaces and hence a greater volume of engineering experience. Figure 1 shows a typical electric furnace dimensioned following the arc furnace electrode spacing rules of Yonemochi [11] and the bath dimensioning rules of Eric [12], which yield an electrode circle pitch diameter (CPD) of precisely three electrode diameters (CPD=3D_e) and a bath diameter of 8.6D_e.

A CPD=3D_e yields a centre-to-centre electrode spacing of ~2.6D_e. If the electrode active areas are 2D_e in diameter as postulated by Wowk [13] and discussed in some detail elsewhere [9], they will form separate zones as shown in Figure 1 (a). If the electrode active area is 3D_e in diameter, as assumed by Yonemochi, the zones will become joined as seen in Figure 1 (b). The joining of active areas can have detrimental effects on crater mechanical stability in some furnaces operating with primarily arc power, but should have fewer consequences for processes that are primarily bath power driven.

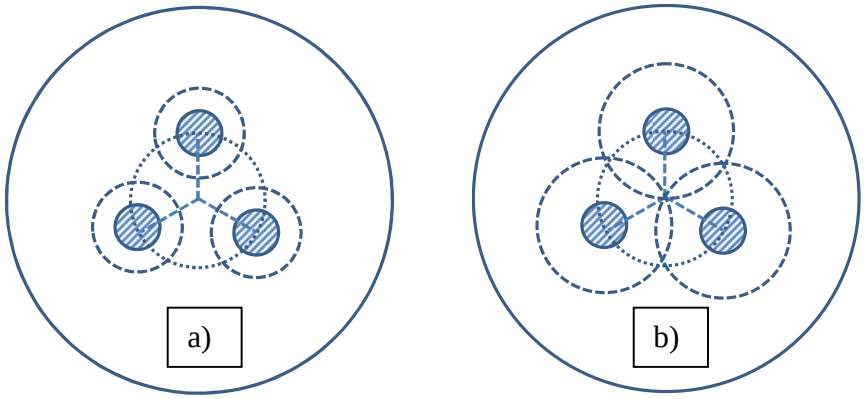

Figure 1. Typical round furnace dimensions, with an 'active' electrode area shown with 'coarse' dotted circles as (a) 2D_e [13] and (b) 3D_e [11], a CPD of precisely 3.0D_e (electrode spacing of ~2.6D_e) [11] shown as a 'fine' dotted line, and a bath dimension of 8.6D_e [12].

Conversion of Electrical Energy into Heat

Thermal energy is released in electric furnaces by the passage of current through resistances. The location of electrical resistances, and therefore voltage drop and heat generation, are critical to correct furnace dimensioning and to the design of feed distribution systems for efficient heat transfer and low losses. For example, it is necessary to ensure that sufficient space is present between the heat-producing-area (HPA) and the wall to slow rapidly moving slag and recover energy by heat-transfer to charge or via endothermic reactions [9]. The size of the active electrode area varies as indicated in Figure 1, and has been reported to be related to the main mode of heat generation, i.e. arc or bath power [6].

Furnace power is often divided crudely into 'arc' and 'bath' power as shown in Equation (1). More realistic modelling of heat development requires careful study of the physics of current flow, the specific nature of the electrical impedances and how they change with temperature, current, process intensity, electrical frequency, etc.:

- Plasma resistivity vs. current and gas type,
- Anode and cathode voltages,
- Arc length,
- Furnace geometric factors (slag depth and electrode spacing),
- Electrode dimensions (diameter and length),
- Electrode resistivity (graphite, carbon and steel casing if present),
- Electrode-slag interfacial resistances for immersed electrodes,
- Fraction of current transferred by ionic conduction (as opposed to electronic conduction),
- Ionic resistivity of the slag, and
- Contribution of the charge to conduction and heat generation.

The focus of the discussion in this section will be with the role of interfacial resistances in both arc and bath systems. The impact of furnace geometry, electrode dimensions and resistivity, and slag ionic conductivity have been discussed in detail elsewhere [9, 10].

Arc and Bath Power

Where power is generated from both arc and slag bath resistance, it is appropriate to separate these inputs, as they typically generate different amounts of slag superheat ($T_{slag} - T_{liquidus}$) and hence slag zone heat losses or refractory erosion [14]:

$$P_{e-total} = P_{arc} + P_{bath} \tag{1}$$

where $P_{e\text{-}total}$ is the total power input (W) of one electrode, i.e. $I_e^2 R_e$, P_{arc} the portion of the power produced in the arc including the heat generated at the anode and cathode spots, i.e. $I_e^2 R_{arc}$ [15], and P_{bath} the power produced by one electrode in the slag bath, i.e. $I_e^2 R_b$, which is typically assumed to be pure joule resistance heating, although it may include interfacial resistances. Total furnace power is then the total power for one electrode, $P_{e\text{-}total}$ multiplied by the number of electrodes used in the furnace design.

Arc physics are beyond the scope of this document, however, the high voltage drops for short arc lengths, i.e. 'brush arc', are worthy of note [16]. The benefits of 'brush' arc in increasing furnace impedance and power input at constant current without adding significantly to slag superheat, have long been known [17]. Brush arc can roughly double the furnace impedance compared to only slightly immersed electrode operation [18].

Interfacial Resistances

For furnaces operating with immersed electrodes, dip tests are often performed to determine the furnace resistance as a function of immersion [18]. Electrode-bottom electrical resistance is found to vary inversely with increased electrode immersion and hence interfacial area, as seen in Figure 2 [22].

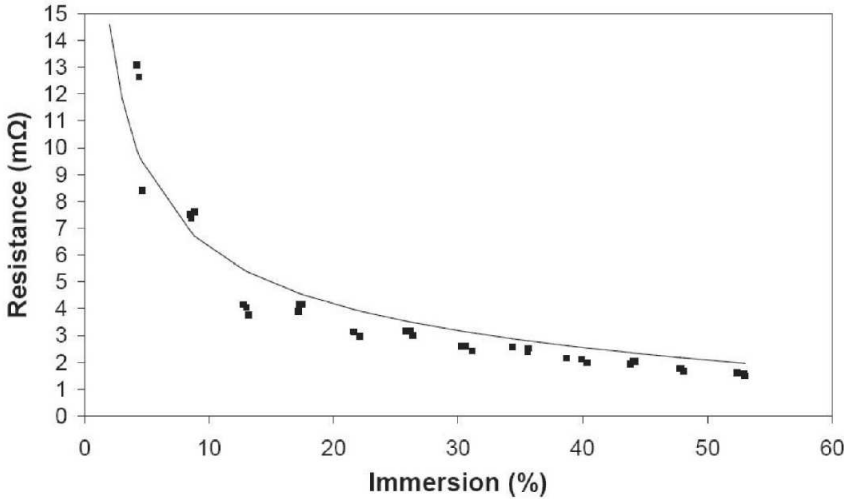

Figure 2. Dip Test Results for Lonmin's furnace number 1 [22].

Data are often misinterpreted by focusing on the depth of the electrode tip from the furnace bottom, perhaps due to the use of 'wye' electrical instrumentation (typically referenced to an artificial bottom contact in AC furnaces) for the control of electrode immersion. Slag furnaces usually behave as if 'infinitely' deep until the electrode is in close proximity to an electrically conductive bottom [10, 18]. The 'delta' electrical model of Downing and Urban [23] is consistent with an infinite conducting medium, and has recently been shown to yield superior results to modern 3D finite element modelling of furnace resistance using the physics of ionic conduction, i.e. without the inclusion of 'contact resistances' [10]. The performance of the Downing and Urban model is also consistent with a higher than expected voltage gradient at the electrode-slag interface, and the presumption of a substantial interfacial resistance (or impedance), which is minimized by larger electrode-slag interfacial area.

If contact resistances dominate furnace resistance, then models focusing on either the electrode height above the bottom (wye) or on the electrode-electrode spacing (delta) will both give less accurate predictions than models related to electrode-slag interfacial area. Where contact resistances do exist, power density will be large and voltage gradients will be steep. Endothermic reactions, e.g. reduction or fuming, will be highly localized in such regions.

Evidence from the few actual furnace measurements available implies that large voltage drops may be present at the electrode interface [9, 14, 19, 20]. This voltage drop may be due to gas at the interface [19] or be related to the creation of ionic concentration gradients, double layers or other frequency dependent 'capacitive' effects [21].

Measurements of graphite (electrode) reactivity and temperature versus electrode-power density in the range of 200-1700 kW/m^2 have shown rapid increases in the rate of reaction of electrodes with FeO in Fayalite slag (producing CO and CO_2 at the electrode-slag interface) [24]. Dramatic increases in electrode temperature compared to the bath temperature were observed with higher power density, implying a significant interfacial resistance may exist between graphite and the Fayalite [24]. The presence of gas at the interface likely results in a positive reinforcement of any initial contact resistance. Gas bubbles of CO and CO_2 are well known to create interfacial resistances in aluminum electrolysis [25]. Søderberg electrodes operate with lower current density than graphite electrodes and therefore have a correspondingly larger interfacial area for any given immersion depth. This larger interfacial area may be an advantage in reducing contact resistances, local voltage/power gradients and hence electrode consumption due to overheating of the carbon surface.

Archibald and Hatch reported that furnace resistance in arcing slag systems includes "contact resistances that are substantially independent of slag depth" and which render the total resistance relatively independent of bath depth, as shown in Table II [14].

Table II. Bath Resistance versus Depth of Slag for a 6 MW Pilot Arc Furnace, D_e=0.46 m (18") and Electrode Centre-Centre Spacing of 1.22 m (4 ft) [14].

Depth (cm)	Bath Resistance (mOhms)
10	20
20	28
30	32
40	33
50	34

Electrode Spacing and Possibilities for Geometric Optimization

If interfacial resistances in low frequency (50/60 Hz) AC or DC furnaces can be proven to exist and their magnitude quantified, electrode spacing and overall furnace dimensions can be reduced, saving capital and reducing total furnace heat losses (less area), at least in furnaces where charge conductivity can be neglected. Alternatively, the same ratio between electrode diameter and bath diameter can be used (e.g. $8.6D_e$) and more slag-charge interfacial area created between the heat-producing-area [9] and the cooled sidewalls. This extra room can be used to 'scavenge' energy to perform 'work', prior to hot slag impinging on cooled sidewall panels where much of the remaining thermal energy will become 'losses'.

Minimum electrode spacing, particularly in low resistance AC furnaces with high currents and strong magnetic fields, will be partly determined by the proximity effect [26]. Inductive phenomena (electromagnetic penetration depth) already result in practical limits on Søderberg

electrode diameters, which are of the order of 2 m [27]. These detrimental effects can be avoided by the use of DC power, which gives greater flexibility for both electrode size and spacing [28].

Charge conductivity can be of primary importance, as in so-called 'coke bed' furnaces used for FeMn production [29], and has now been shown as a potential factor in many furnaces formerly thought to operate as pure arc processes [30]. Where charge conductivity is an important factor, furnaces may actually benefit from larger electrode spacing, as this will permit the use of longer arcs and correspondingly reduced bath power, due to lower current for a fixed electrode power.

Heat Transfer and Energy Losses

Higher furnace power intensity implies a smaller furnace for the same total power input as mentioned previously. Typically this results in lower total energy losses, even though it usually results in higher sidewall heat fluxes [6, 9]. A smaller furnace must melt more material per unit area per unit time, for the same total power input. Higher heat transfer between the slag and the charge is required, and this is typically supplied by greater slag superheat (assuming a fairly constant heat transfer coefficient), as indicated by Equation (2).

$$Q_{slag\text{-}charge} = A_{slag\text{-}charge}\, h_{slag\text{-}charge}\, (T_{slag} - T_{liquidus}) \qquad (2)$$

where: $Q_{slag\text{-}charge}$ is the amount of thermal energy per unit time that must be transferred to heat, drive endothermic reactions, and melt the charge [W], $A_{slag\text{-}charge}$ the interfacial area between slag and charge [m^2], $h_{slag\text{-}charge}$ the overall slag-to-charge heat transfer coefficient ($W/m^2 \cdot K$), T_{slag} the average temperature of the bulk slag under the charge [K], and $T_{liquidus}$ the liquidus temperature of the slag [K]. The required bulk slag temperature will be reduced to the extent that endothermic reactions take place in the liquid rather than the solid state.

Impact of Arc Power

The use of arc power as described in Equation (1) allows energy to be transferred directly to the solid charge without necessitating heating of the slag, thereby reducing the required magnitude of $Q_{slag\text{-}charge}$ for a fixed total furnace power and hence reducing the required slag temperature and superheat [14, 17]. In analyzing furnace power intensities and how they relate to slag bath heat losses, it is possible in many instances to subtract the total arc power from the total furnace power, and relate the wall heat losses to the total bath power intensity alone, i.e. $P_{total\ bath}/m^2$.

In the case of open bath processes, heating by arc power must take place either while the material is 'in-flight' or by directly feeding the arc attachment spot on the slag surface. Finely divided feed with a high surface to volume ratio and low settling velocity would be expected to reduce furnace energy losses by more efficiently absorbing radiation as the feed falls through the freeboard (increasing opacity and reducing radiation losses). A higher degree of feed preheating in the freeboard will reduce the required slag superheat, and therefore the sidewall heat losses.

In covered bath processes, energy can be transferred from an electrode 'cavity' to charge banks, as in the case of a choke fed furnace design. Deep charge banks surrounding long arcs (high

proportion of P_{arc}) should therefore reduce furnace wall and freeboard energy losses. Charge banks also facilitate drying, heating and pre-reduction of the feed by allowing hot gases produced in the slag to rise up through the incoming feed material. This reduces the total energy that must be supplied by convective heat transfer from the hot slag and hence the required slag superheat. Choke fed furnaces typically require 'coarse' feeds to ensure sufficient charge permeability. The required permeability is related to the total volume flux of gas produced in the slag and therefore to the amount of reduction performed. Semi-open bath is sometimes used for difficult feeds, allowing the electrode 'delta' to partially open to release gases formed in the liquid bath [31].

Impact of Bath Power

When higher process intensities are driven by increased bath power and slag superheat, hotter slag arrives at the walls, and results in a greater loss per unit area. The slag-wall heat flux [W/m^2] can then be calculated from equation (3).

$$Q/A_{\,slag\text{-}wall} = h_{slag\text{-}wall}\,(T_{bulk\,slag} - T_{hotface}) \tag{3}$$

where $Q_{\,slag\text{-}wall}$ is the rate of wall heat loss [W], $A_{\,slag\text{-}wall}$ the area of the coolers [m^2], $h_{slag\text{-}wall}$ the slag-to-wall heat transfer coefficient [W/m^2·K], $T_{bulk\,slag}$ the temperature of the bulk slag close to the wall [K] and $T_{hotface}$ the temperature at the mushy zone at the panel hot-face [K], which can be taken as the average of the liquidus and solidus of the slag [32].

Heat transfer from slag to charge and walls was well described by Bendzsak and Baines in terms of five heat transfer zones [33]. Slag heated near the electrode produces buoyancy driven flows, which convect energy to the slag-charge interface. Hot slag then moves under the charge towards the wall. It was postulated by Bendzsak and Baines that immediately adjacent to the wall there exists a stagnant slag layer undergoing natural convection heat transfer. Kang and Robertson performed experimental work with waxes, and found that the heat transfer of slag at walls could be adequately described by a correlation for a vertical plate undergoing natural convection [34]:

$$Nu_{slag-wall} = 0.32\left(Gr_{slag-wall}\,Pr_{slag}\right)^{0.3} \tag{4}$$

where $Nu_{slag\text{-}wall}$ is the Nusselt number at the slag-cooler interface [unitless], $Gr_{slag\text{-}wall}$ the Grashof number [unitless], and Pr_{slag} the Prandtl number [unitless].

$$Nu_{slag-wall} = \frac{h_{slag-wall}L}{k_{slag}}, (5) \qquad Gr_{slag-wall} = \frac{g\rho_{slag}^2\beta\left(T_{bulk\ slag} - T_{hotface}\right)L^3}{\mu_{slag}^2}, (6) \qquad Pr_{slag} = \frac{C_p\mu_{slag}}{k_{slag}}, (7)$$

where $h_{slag\text{-}wall}$ is the natural convection heat transfer coefficient at the melt-cooler interface [W/m^2·K], L is a characteristic length, i.e. the height along the cooler [m], k_{slag} the thermal conductivity of the molten material [W/m·K], g the acceleration due to gravity, 9.81 [m/s^2], ρ_{slag} the melt density [kg/m^3], β the melt volumetric expansion coefficient [m^3/m^3·K], μ_{slag} the viscosity [Pa·s] and C_p the heat capacity of the melt [J/kg·K].

Equation (4) has been found to be adequate to predict 'nominal' sidewall cooler heat losses in actual slag furnaces [9, 32], which are often in the range of 10-100 kW/m^2, with typical values in the range of 10-50 kW/m^2 in the case of ferronickel smelting [6]. For low iron, high silica slag in ferronickel smelting, superheats are typically the range of 50 [35] - 150 ^{o}C [36], implying a slag-wall heat transfer coefficient of the order of 300 W/m^2·K.

Emergency Conditions and Required Safety Factors

Equation (4) is only valid where the assumption of a natural convection boundary is true. 'Reversion' reactions have been reported in the literature [6, 37] where dissolved silicon or carbon in a highly reduced metal phase is brought in contact with an overly oxidized slag and rapidly re-equilibrates or 'reverts', releasing energy (silicon reversion), and gas (carbon reversion). The combination of energy with gas stirring can lead to very high local heat fluxes in the vicinity of sidewall coolers. In order to protect coolers against such events, it is necessary to design them with very large safety factors. Safety factors should be based on the analysis of past data where available, considering the mean and about 4-5 standard deviations in the observed heat fluxes. A modern copper cooler with a hot face pattern and large internal heat transfer surface area, is shown in Figure 3.

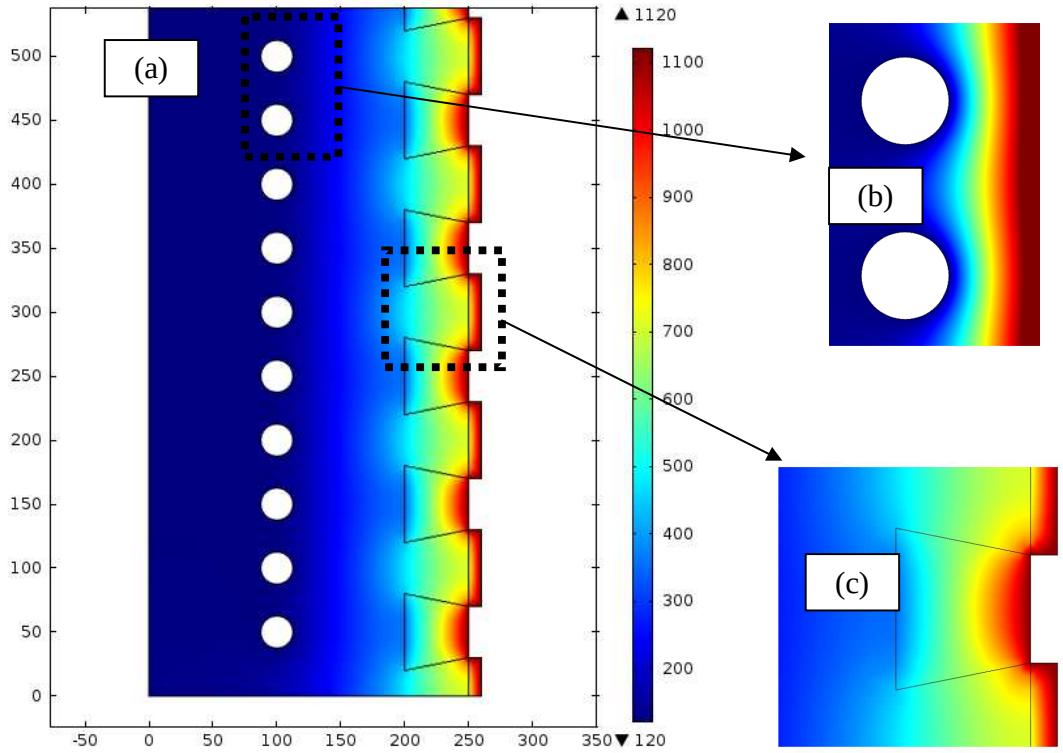

Figure 3. (a) Simplified 2D FEM model of a furnace cooler (half section shown) at steady state, simulating a critical 'emergency' heat flux of 1 MW/m^2, ~1100 ^{o}C hot face temperature, 10 mm of frozen slag on the copper, and exposed refractory lined dove-tail grooves on the hot face. (b) Close up of a cooler, where the color scale has been modified such that red indicates 200 ^{o}C and dark blue 120 ^{o}C. (c) Close up of one refractory lined pocket showing incipient melting of the copper in the corners at the hot face [38].

The copper block shown in Figure 3 is modelled with a hot face heat flux of 1 MW/m^2 and the results indicate incipient copper melting on the hot face. Coolants and cooling systems have been extensively reviewed elsewhere [38].

Impact of Process and Operating Practices on Energy Losses

Furnace operators tend to blame furnace designers for excessive energy losses and fail to acknowledge the role that operating practices have on process efficiency. The second law of thermodynamics ensures that any 'mistake' or deviation from optimal operation will decrease process efficiency and in the case of slag furnaces increase energy losses, e.g.:

1. Failure to maintain the correct ratio of feed-to-power on a short term basis for a furnace with a 'free-burning' arc or an open bath with low solid inventory, will result in excessive radiation and sidewall energy losses.
2. Under feeding of the 'hot-spot' near the electrodes will cause the bath to open and increase radiation losses to the upper-wall and roof.
3. Insufficient wall 'dressing' will tend to allow hot slag to directly impinge on the sidewall coolers increasing local heat losses.
4. Incorrect electrode positioning for the given feed characteristics will result in either overheated matte/metal (electrodes too low) or opening of the bath surface (electrodes too high).
5. Too many fines in the feed will reduce charge porosity and increase the smelting rate of the feed, preventing the use of choke feeding and result in more open bath-like conditions and higher radiation losses.
6. Too much reduction duty will produce excessive gas and may require that the bath be opened to avoid slag foaming; hence, increasing radiation losses.
7. Presence of solid particles in the slag will increase the effective viscosity, (e.g. Chromite - Cr_2O_3) forming high melting spinels, and require greater superheat to maintain slag fluidity.
8. Excessively pure feed may cause 'melting' to become mass-transport limited and not heat-transport limited, i.e. to become dissolution rather than melting.

Point 8 is worthy of further discussion. From a thermodynamic standpoint there is not a great deal of difference between melting simple compounds or mixtures of such compounds. In fact, due to the heat of mixing, it is theoretically preferred to begin with pure feeds, for example FeO and SiO_2, rather than 'mixtures' like Fayalite. Smelting of a 2:1 mole ratio of FeO and SiO_2 in either form, will successfully operate with 100-150 ^oC of superheat over the melting point of Fayalite, e.g. a temperature of about 1250 ^oC; however, the two cases will function with very different efficiencies. The pure feed case will be mass-transfer and not heat-transfer limited. With the melting point of pure SiO_2 being over 1600 ^oC, it is clear that pure SiO_2 will never melt at 1250 ^oC, and must therefore be dissolved in the slag. Stirring and particle-size/interfacial area will then strongly impact the rate of 'melting', the steady-state slag superheat, and hence the sidewall heat losses. Furnace models which use the feed 'average' composition, rather than the melting point of the individual feed particles, are therefore unlikely to be accurate predictors of furnace thermal efficiency.

Volumetric Reactions and Maximum Useable Power Intensity

If it is accepted that slag superheat is the primary driver of furnace slag zone heat losses, then reactions which absorb energy on a volumetric basis should by their nature, reduce furnace losses. Many commercial smelting processes utilize the vast majority of the input electrical energy to melt charge, rather than to reduce or fume. Such processes will therefore have a nearly linear increase in slag superheat for increased bath power intensity. In the case of ferronickel it has recently been shown that less than 10% of the input electrical energy goes to drive bath reduction reactions [6]. This balance showed that for a total power intensity of only 350 kW/m^2 (and perhaps 100-175 kW/m^2 of bath power), a sidewall heat loss of 25 kW/m^2 was expected to result.

Eras Metal A.S. operates a submerged plasma fired zinc fuming process at a smelter located in Høyanger Norway. This process uses three plasma burners supplied by Scan Arc Plasma Technology A.B., in a double jacked steel water-cooled furnace, similar in general layout to an Aus- or ISASMELT vessel, and with a ~1.8 m internal diameter hearth. A similar submerged plasma fired fuming process has been described in the literature [39].

In the process operated at Eras, air is heated by the plasma burners each typically running at 2-2.5 MW. The plasma is then mixed with natural gas and additional air and injected at ~3000-4000 K and supersonic velocity into the liquid bath, which is typically at 1250-1350^oC. A mixture of moistened EAF dust, whole alkaline batteries, green petroleum coke and silica flux is fed via the top of the furnace at a rate of about 6-7 wet mt/h and falls directly into the plasma agitated bath. Zinc is reduced and fumed as metal vapour and subsequently re-oxidized to a high grade zinc powder product. Iron units in the feed are converted to FeO and fluxed with silica and lime (from the EAF dust), and tapped as a high density and environmentally stable FeO-rich iron-silicate.

The process at Eras operates with a total net power input from the plasma units (chemical and electrical) of about 2.5 MW/m^2 of hearth area or about 1.7 MW/m^3 of bath volume (1.3 MW/m^3 of electrical power only) making it a High or Ultra-High intensity process according to Elkem's definitions, given previously in Table I. Of the total power input, only 14% is lost through the water cooled shell, at an average of <20 kW/m^2. Heat losses in the most heavily agitated areas are in the range of 30-70 kW/m^2, depending on location and operating conditions. Considering the violence of the bath agitation, the low magnitude of the losses defies conventional wisdom of what can be accomplished in a bath smelting process.

To explain the combination of extreme agitation, small diameter furnace, ultra-high power intensity and low heat losses, it is necessary to examine how energy is used within the vessel. Detailed mass and energy balances performed using HSC Chemistry®, show that of the total net power added to the bath via the plasma units, approximately 50% is used in 'volumetric' reduction and fuming reactions. Subtracting this power from the total supplied to the vessel still leaves an impressive power intensity of 1.25 MW/m^2. Fine feed, large gas-liquid interfacial area, and strong inter-phase mixing, must also contribute in large part to the efficient operation with low bath superheat, which is typically on the order of 50-150^oC.

Conclusions and Recommendations

Increased understanding of the physics of slag furnaces will enable improvements in both design and operation.

Design of optimized slag processes requires further study particularly in the areas of:

- Electrical conduction in and energy transfer to: slag and charge, under low frequency conditions,
- Mechanisms of heat losses from superheated slag to side wall, and
- The role of reduction and fuming reactions as volumetric heat sinks, and their impact on maximum usable power intensities.

Accurate heat transfer modelling of slag furnaces will not be possible without accurate electrical models. Accurate electrical models require the inclusion of all of the necessary physics. Experimental work appears to be warranted to elucidate the voltage gradients in close proximity to electrodes in both molten slag and within the charge bed of choke fed furnaces. Such experimental work, particularly if conducted at variable frequencies, may provide a better idea of the nature of the real interfacial resistances, including any possible capacitive effects.

Lack of understanding can lead to good furnace designs being operated with poor efficiency. Optimal operation requires the correct appreciation of where thermal energy is developed and how to accomplish efficient heat transfer for melting, fuming, and/or reduction.

References

1] G. Kleinschmidt, R. Degel, M. Köneke, and H. Oterdoom, "AC- and DC- Smelter Technology for Ferrous Metal Production," *The Twelfth International Ferroalloys Congress*, (2010) 825-838.

[2] J. P. Kapusta, "JOM World Nonferrous Smelters Survey, Part I: Copper," *Journal of Metals*, vol. 56, (2004), 21-27.

[3] A. Warner, C. Díaz, A. Dalvi, P. Mackey, and A. Tarasov, "JOM World Nonferrous Smelter Survey, Part III: Nickel: Laterite," *Journal of Metals*, vol. 58, (2006), 11-20.

[4] G. G. Richards, J. Brimacombe, and G. Toop, "Kinetics of the Zinc Slag-Fuming Process: Part I. Industrial Measurements," *Metallurgical Transactions B*, vol. 16, (1985), 513-527.

[5] R. T. Jones, "JOM World Nonferrous Smelter Survey, Part II: Platinum Group Metals," *Journal of Metals,*, vol. 56, (2004), 59-63.

[6] C. Walker, T. Koehler, N. Voermann, and B. Wasmund, "High Power Shielded-Arc FeNi Furnace Operation-Challanges and Solutions," *The Twelfth International Ferroalloys Congress*, (2010), 681-696.

[7] M. W. Kennedy, H. Haaland, and J. A. Aune, "High Intensity Slag Resistance Furnace Design," *Pyrometallurgy of Nickel and Cobalt*, (2009), 101-111.

[8] K. Verscheure, A. K. Kyllo, A. Filzwieser, B. Blanpain, and P. Wollants, "Furnace Cooling Technology in Pyrometallurgical Processes," *Sohn International Symposium, Advanced Processing of Metals and Materials, Vol 2.*, (2006), 139-154.

[9] M. W. Kennedy, "Electric Slag Furnace Dimensioning Criteria," *International Smelting Technology Symposium*, (2012), 279-290.
[10] M. W. Kennedy, M. Garcia, and F. Olesen, "Comparison of Classical Tools and Modern Finite Element Modeling in the Electrical Design of Slag Resistance Furnaces," *International Smelting Technology Symposium*, (2012), 239-249.
[11] J. Yonemochi, "Basic Concepts in the Electric Smelting of Ferroalloys," *Electric Furnace Conference*, (1976), 73-77.
[12] R. Eric and A. Hejja, "Dimensioning, Scale-up and Operating Considerations for Six Electrode Electric Furnaces. II. Design and Scale-up Considerations for Furnaces Treating PGM-Containing Copper-Nickel Concentrates," *EPD Congress*, (1995), 239-257.
[13] Z. B. Wowk, "Characteristics of a Submerged-Arc Furnace," *Electric Furnace Conference*, (1964), 158-160.
[14] F. R. Archibald and G. Hatch, "Electric Arc Furnace Operation," US Patent 3,715,200, 1973.
[15] G. Sævarsdottir, M. T. Jonsson, and J. Bakken, "Arc-Electrode Interactions in Silicon and Ferrosilicon Furnaces," *Tenth International Ferroalloys Congress*, (2004), 593-604.
[16] J. McKelliget and J. Szekely, "A Mathematical Model of the Cathode Region of a High Intensity Carbon Arc," *Journal of Physics D: Applied Physics*, vol. 16, (1983), 1007-1022.
[17] A. A. Dor, and H. Skretting, "The Production of Ferronickel by the Rotary Kiln-Electric Furnace Process," *International Laterite Symposium*, (1979), 459-490.
[18] B. Boulet, V. Vaculik, and G. Wong, "Control of Non-Ferrous Electric Arc Furnaces," *American Control Conference*, (2003), 3060-3064.
[19] Y. Sheng, G. Irons, and D. Tisdale, "Transport Phenomena in Electric Smelting of Nickel Matte: Part I. Electric Potential Distribution," *Metallurgical and Materials Transactions B*, vol. 29, (1998), 77-83.
[20] M. Manvelyan, A. Melik-Ankhazaryan, K. Kostanyan, and S. Nalchadzhyan, "The Use of Graphite Electrodes in Electrically Heated Glass Furnaces," *Glass and Ceramics*, vol. 13, (1956), 297-303.
[21] N. A. Fried, K. G. Rhoads, and D. R. Sadoway, "Transference Number Measurements of TiO_2–BaO Melts by Stepped-Potential Chronoamperometry," *Electrochimica acta*, vol. 46, (2001), 3351-3358.
[22] G. Georgalli, J. Eksteen, R. Bezuidenhout, B. Van Beek, and T. Goff, "Towards Electrode Immersion Control on Lonmin's No. 1 Circular Furnace," *Journal of the South African Institute of Mining & Metallurgy*, vol. 109, (2009), 219-230.
[23] J. Downing and L. Urban, "Electrical Conduction in Submerged Arc Furnaces," *Electric Furnace Conference*, (1965), 93-101.
[24] K. El-Rassi and T. Utigard, "Rate of Slag Reduction in a Laboratory Electric Furnace—Alternating Vs Direct Current," *Metallurgical and Materials Transactions B*, vol. 31, (2000), 1187-1194.
[25] M. A. Cooksey, M. P. Taylor, and J. J. Chen, "Resistance Due to Gas Bubbles in Aluminum Reduction Cells," *Journal of Metals*, vol. 60, (2008), 51-57.
[26] H. Larsen, "Current Distribution in the Electrodes of Industrial Three-Phase Electric Smelting Furnaces," *Proceeding of the 2006 Nordic COMSOL Conference*, (2006), 1-4.

[27] J. Westly, "Critical Parameters in Design and Operation of the Submerged Arc Furnace," *Electric Furnace Conference*, (1975), 47-53.
[28] I. Barker, "Some Considerations on Future Developments in Ferroalloy Furnaces," *Journal of the Southern African Institute of Mining and Metallurgy,* vol. 111, (2011), 691-696.
[29] M. Dhainaut, "Simulation of the Electric Field in a Submerged Arc Furnace," *Proceedings of the Tenth International Ferroalloy Congress*, (2004), 605-613.
[30] A. Shkirmontov, "Establishing the Theoretical Foundations and Energy Parameters for the Production of Ferroalloys with a Larger-Than-Normal Gap under the Electrode," *Metallurgist,* vol. 53, (2009), 300-308.
[31] S. Barnett, I. Patino, and F. Perez, "Smelting of Lateritic Nickel Ore at Cerro Matoso S. A., Colombia," *Extraction Metallurgy'85*, (1985), 877-890.
[32] H. Joubert, "Designing for Slag 'Freeze Linings' on Furnace Sidewalls – an Engineering Perspective," *Molten Slags, Fluxes and Salts*, (2000), 1-11.
[33] G. Bendzsak and W. Baines, "Analysis of Heat and Mass Transfer Mechanisms in Electric Smelting Furnaces," *International Symposium on Non-ferrous Pyrometallurgy: Trace Metals, Furnace Practices and Energy Efficiency*, (1992), 23-27.
[34] S. Kang, "A Model Study of Heat Transfer and Fluid Flow in Slag-Cleaning Furnaces," *Dissertation Abstracts International (USA),* vol. 52, (1992), 1-182.
[35] N. Voermann, T. Gerritsen, I. Candy, F. Stober, and A. Matyas, "Developments in Furnace Technology for Ferro-Nickel Production," *INFACON X*, (2004), 1-11.
[36] F. Stober, T. Miraza, A. T. Hidyat, I. Jauhari, K. Belanger, D. Fowler, T. Gerritsen, A. Matyas, C. Nichols, and N. Voermann, "Furnace Upgrade with Hatch Technology at PT Antam FeNi-II in Pomalaa, Indonesia," *INFACON XI*, (2007), 638-653.
[37] L. Nelson, R. Sullivan, P. Jacobs, E. Munnik, P. Lewarne, E. Roos, M. Uys, B. Salt, M. de Vries, and K. McKenna, "Application of a Highintensity Cooling System to Dc-Arc Furnace Production of Ferrocobalt at Chambishi," *Journal of the South African Institute of Mining and Metallurgy*, vol. 104, (2004), 551-561.
[38] M. W. Kennedy, P. Nos, M. Bratt, and M. Weaver, "Alternative Coolants and Cooling System Designs for Safer Freeze Lined Furnace Operation," *Nickel-Cobalt 2013*, (2013) 299-314.
[39] K. Verscheure, M. Van Camp, B. Blanpain, P. Wollants, P. Hayes, and E. Jak, "Continuous Fuming of Zinc-Bearing Residues: Part II. The Submerged-Plasma Zinc-Fuming Process," *Metallurgical and Materials Transactions B*, vol. 38, (2007), 21-33.